Analysis of Flat Panel Speakers

Luke Humphry
King's College

Fourth-year undergraduate project in Group C

2006/2007

I hereby declare that, except where specifically indicated, the work submitted herein is my own original work.

Signed:_____ Date:_____

Technical Abstract

The flat panel speaker is a relatively new technology that disregards the normal rules of loudspeaker design by encouraging resonance in the speaker cone. These speakers have been commercially available for some 10 years, yet little is known about their method of operation. A single company (NXT) licenses flat panel speaker technology to manufacturers, but has given scant explanation as to how these devices work. Though there is beginning to be academic interest in these speakers, current computational techniques (Finite Element Analysis, Boundary Element Method) are extremely slow when analysing vibrating panels with such high degrees of freedom. Due to the slow nature of these methods it has not been possible to perform investigative research to understand the method of operation of such panels. By using a new computational method that describes the surface displacement of the panel using Jinc function wavelets, the radiated power spectrum can be computed for a panel in a fraction of time previously needed. Using this method it has been possible to fully analyse flat panel speakers and for the first time provide an explanation for how they work to the academic community.

To analyse the acoustical properties of a flat panel speaker, a computer simulation of such a device was designed and built within MatLab. This model contains two distinct submodels – 1) a simulation of the structural dynamics of a flat panel speaker, and 2) a prediction of the power radiated from the surface of this panel when coupled with surrounding air. Both submodels contain simplifying assumptions about the nature of panels being simulated, but due the separate nature of the submodels it is a simple procedure to add in more complexity to one area of the model in the future. For a typical flat panel speaker the complete model can compute a 4000 point power spectrum over the working range (20Hz – 20kHz) in approximately 3 hours. Until recently this would have taken many days.

This model was used to compute the power spectrum of a real flat panel speaker. The speaker was dismantled and its panel carefully measured to find out all the parameter values need to run the model. The panel was found to have high damping and high modal density, and critical frequency of 23kHz, above the working range of the speaker. The resulting power spectrum was found to be extremely flat above low frequencies. By changing the damping of the simulated panel and computing the radiated

power spectrum for different damping values, it was found that the real panel was close to radiating like an infinite panel, with no wave/boundary interactions. For this behaviour the driving point radiates all acoustic power, acting like a monopole. The real panel radiated power approximately 3x in magnitude that of an infinite plate. The difference was found to be due to a reverberant bending-wave field in the panel area around the drive point. An approximate value for the radiation from this reverberant field was calculated using Statistical Energy Analysis (SEA), and when added together with the power radiated from the drive point gave extremely close agreement with the model predicted power spectrum. These two methods of panel radiation are normal not seen together, but the combination of high damping (producing infinite plate behaviour), high modal density (creating a reverberant field), and being below the critical frequency (meaning no dominant modes) results in both radiation sources being present in this case. Both sources of radiation have a highly dispersed pattern, a known feature of flat panel speakers. The dual radiation theory was validated by calculating the SEA approximate power spectrum of other flat panel speakers and then checking with results predicted by the full Jinc function model. Excellent agreement was seen for a range of panels.

The method of operation of a single pair of flat panel speakers is now understood, and this dual radiation method is thought to hold for a wide range of flat panel speakers. The SEA approximation provides an extremely quick way of computing the approximate radiated power spectrum for a flat panel speaker (<15minutes). This approximation is typically within 3dB of the true value due to the flat nature of the true spectrum and so is accurate enough for most purposes. The SEA approximation is a new tool in flat panel speaker design and due to its speed allows for new design methods, namely optimisation.

Contents Page

Section 1: Introduction

1.1 Background

1.1.1 Conventional Loud Speakers

Electrically powered loudspeakers have existed for over 100 years, and are omnipresent in our lives – we find them in laptops, radios, mobile phones, train address systems to name only a few. Conventional loudspeakers rely on piston-like cones to provide the mechanical motion that creates sound waves. This is not new technology – it was in 1925 that C. Rice and E. Kellogg first devised the piston-cone arrangement that dominated loudspeaker design for the rest of the 20th century. Much academic and commercial effort has gone into making these cones as rigid as possible through improved materials and adhesives, eliminating any resonances. These resonances are the main cause of unwanted audio colouration and 'smear'.

Despite the age of this technology the design is by no means perfect and piston-cone loudspeakers suffer from one key problem: at high frequencies the sound radiated tends to become very directional – they 'beam'. This means that it is extremely difficult to evenly fill a space with sound radiated from conventional speakers, especially given the variations in directivity at different frequencies.

1.1.2 Distributed Mode Loudspeakers

10 years ago the first 'Distributed Mode' loudspeakers (DMLs) were developed by New Transducers Ltd (known as NXT). These speakers turn convention on its head by actively encouraging resonances in the loudspeaker cone. A thin flat panel is used and is generally excited using a magnetic coil to set up bending waves throughout the panel. These DMLs (or 'flat panel speakers' as they are often called) are the first new idea in speaker technology in over 60 years, and have some exciting properties: a very dispersed radiation pattern at all frequencies; and their slender dimension. Figure 1 below shows the dispersed nature of this new technology.

Figure 1 – Typical Radiation Patterns for Conventional and Distibuted Mode Loudspeakers

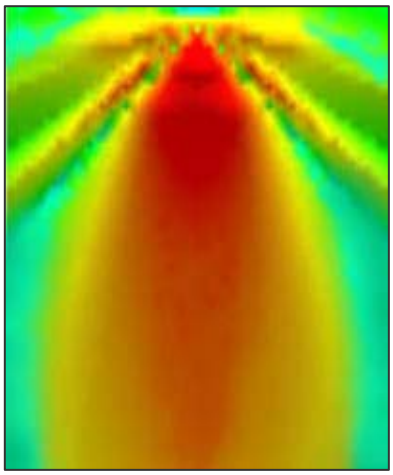

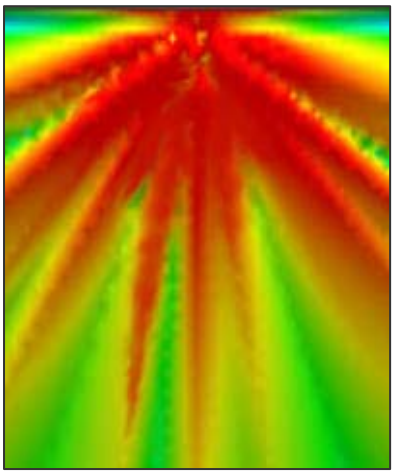

[Images from Elac Electroacoustics Website]

Conventional loudspeakers show a high degree of directivity, 'beaming' at high frequencies.

Distributed mode loudspeakers show a far more dispersed radiation pattern.

The sound quality of flat panel speakers is not yet as good as the best piston-cone speakers, but their slender dimensions and ability to evenly fill a room with sound are resulting in them being used widely for home cinema, computer audio, and public address systems.

1.1.3 Current Understanding of Flat Panel Speakers

Though NXT design and licence DML technology, they give little explanation as to the physics of DML sound radiation. The most in-depth description of the theory comes in NXT's original introductory article for the audio industry [Azima, 1998]. Here they state that by exciting such panels so as to set up bending waves, a series of complex and highly random waves are produced. These waves are so complex as to be almost random, and so each point on the panel acts like a small independent cone radiating uncorrelated sound waves. Due to the complex and uncorrelated nature of resonance, adjacent sound waves do not cancel one another out, and so we observe a very diffuse radiation pattern, approaching that of a point source.

There is beginning to be academic interest in this kind of loudspeaker, but there is not thought to be any further explanation as to how these flat panel speakers work other than that given by NXT. Most academic work has been concerned with novel uses for this technology and not in understanding the underlying physics.

1.2 Motivation for Work

1.2.1 A New Analysis Technique

To analyse a thin walled structure such as a flat panelled speaker it is natural to analyse the air-structure coupling to calculate the sound power radiated into the surrounding air. In the past two decades it has been convention to analyse complex structures using either the boundary element method (BEM) or finite element method (FEM). These methods are well understood and can be applied to a large number of general structures, but even with advances in computing power they remain rather slow. This is especially problematic for high frequency analysis, where short wavelengths necessitate very many degrees of freedom.

A new method has been developed that uses Jinc function wavelets to analyse the power radiated from planar structures [Langley, 2007]. This method is not as general as BEM or FEM but for simple planar structures allows for much faster analysis of the acoustical power radiated from their surface. We shall not discuss the Jinc function method in any depth, but in summary the method is to describe the surface displacement of the structure by using a grid of Jinc function wavelets [see Appendix 1 for description of Jinc function]. These wavelets are radially symmetric, allowing for a simple and analytic calculation of the dynamic stiffness of the structure, from which the radiated acoustic power can also be calculated analytically. It is this analytic nature that allows for much faster computation than all previous methods and suits the analysis of flat panel speakers well.

1.2.2 Explaining the Physics of Flat Panel speakers

Though flat panel speakers have now been on the market for over a decade, there has been no clear explanation for the governing physics. NXT likely understand the physics, but their brief explanation is without any physical or mathematical rigour to back up their claims. These loudspeakers do reproduce sound well, as countless commercial products and reviews testify, but prior to this research no-one in the academic community understood why. NXT are an intellectual property based company, and seem to be working hard to ensure their I.P. is kept secure – to the point where DML license holding manufacturers cannot advertise the full specifications of their DML products. Through use of the fast Jinc function method it was felt that the time was now right to investigate

how these loudspeakers operate and try to provide an explanation to the academic community at large.

1.3 Research Strategy

1.3.1 Designing a Model Speaker

It is rather difficult to analyse DMLs experimentally, as has been documented previously [Hill & Mapp, 2003]. For this research an accurate computer model of a flat panel speaker was designed. Firstly, a model that simulated the structural dynamics of a flat plate was needed – how the plate responds to a given force input. A program was written that simulated the displacement response to a given harmonic force input at any frequency. This model was made to be general enough to allow for many changes in plate properties. To predict the acoustic power radiated from such a plate, the model plate was coupled to the surrounding air space. This involved using the Jinc function method to predict the dynamic stiffness and so the acoustic power.

1.3.2 Investigate real speakers

Having designed an accurate model, a real set of flat panel speakers was dismantled and measured to find out the physical properties of a typical set of flat panel speakers. These properties were fed into the model to allow the acoustic power to be predicted. This led to some interesting discoveries and theories. These theories were investigated and validated by changing various properties of the model speakers and re-analysing the predicted acoustic power output.

1.4 Structure of Report

This report documents the stages of development of the research introduced previously, and the resulting conclusions. The research consisted of 2 main phases, and so shall this report:

1) Designing and building the dynamic response model of a flat panel speaker, and coupling this to the surrounding air
2) Using this model to analyse flat panel speakers

The first section shall give the underlying theory behind the models used, how the theory was implemented, and what investigative tools result from each model. The second section will deal with four issues: how the parameter values of a real flat panel speaker

were found, what results the model predicted for these values, what the implications of these results are, and how any theories about flat panel speakers can be validated. In academic papers it has become common to refer to 'flat panel speakers' as 'distributed mode loudspeakers' (DMLs), and this term shall be used from here on in this document.

Section 2: Building an Accurate Model

2.1 Structural Dynamics Model

2.1.1 Theory

A DML is little more that a flat plate with some boundary conditions given by the frame it rests in. Simply supported plates have the simplest mode shapes of all plates, so it is sensible to begin by modelling this type. The model was designed to be general enough to allow different edge conditions to be imposed in future, with all subsequent parts of the model still performing correctly. A simply supported flat plate has mode shapes and frequencies given by [Crighton et al, 1992, p589]:

$$\phi_{nm}(x,y) = \sin\left(\frac{n\pi x}{L_x}\right)\sin\left(\frac{m\pi y}{L_y}\right), \qquad \omega_{nm}^2 = \left(\frac{D}{\rho h}\right)\times\left[\left(\frac{n\pi}{L_x}\right)+\left(\frac{m\pi}{L_y}\right)\right]^2 \qquad \text{(1a,b)}$$

where L_x and L_y describe the planar dimensions of the plate, h the thickness, ρ the density of the plate material, and D the bending stiffness. The response of this plate to a forced sinusoidal displacement, F, at a point (x_o, y_o), and at some frequency, ω, can be found using a summation of mode shapes:

$$u(x,y) = \sum_n \sum_m \left[\frac{F\phi_{nm}(x,y)\phi_{nm}(x_o,y_o)}{\omega_{nm}^2(1+i\eta)-\omega^2}\right] \qquad (2)$$

where η defines the coefficient of damping of the plate. It is convention to normalise the mode shapes by the system mass before using the infinite summation. All modes were multiplied by a normalising factor before summation:

$$NF = \frac{2}{\sqrt{\rho h L_x L_y}} \qquad (3)$$

2.1.2 Modelling Technique

Using MatLab as our programming environment, it is simple to calculate the mode shapes given by Eqn. (1a) directly. But to compute the panel displacement at any given frequency how do we decide the limits to use for our summation in Eqn. (2), which is in theory infinite?

Using a wavenumber space approach to represent different modes, it is known that for modes close to frequency ω the mode with the maximum n value occurs when m is 1, and vice versa [Norton & Karczub, 2003, p210], see Figure 2 below.

Figure 2 – Modes in Wavenumber Space

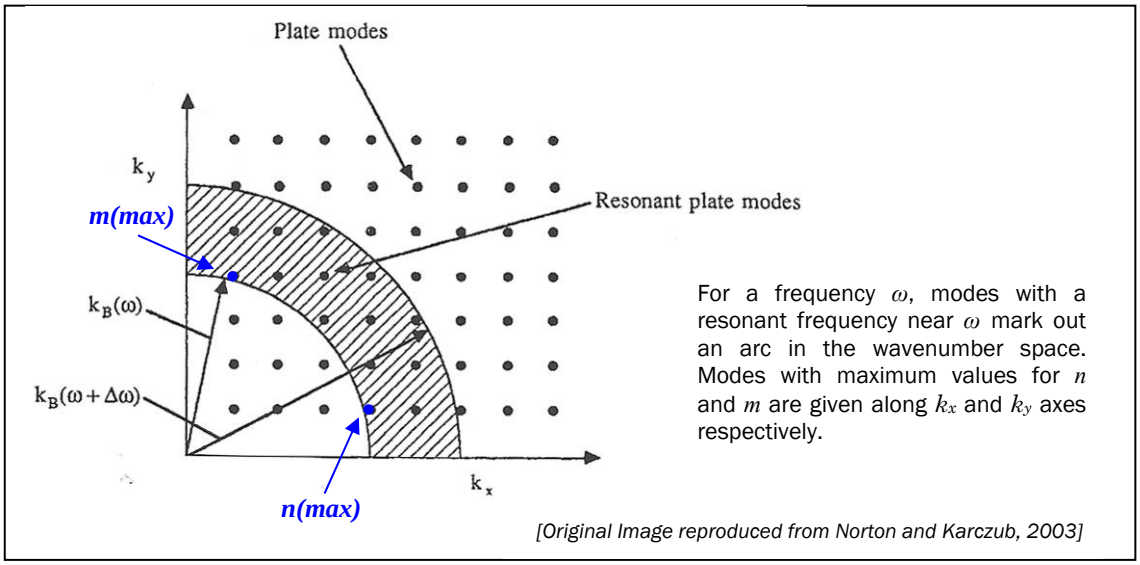

[Original Image reproduced from Norton and Karczub, 2003]

It was found that to calculate the response of the plate one should sum over modes up to and including $\Phi_{1.5n(max),1.5m(max)}$, subsequent modes making no practical difference to the response due to the factor ω_{nm}^2 becoming extremely large and further away from ω^2. The values $n(max)$ and $m(max)$ can be calculated by rearranging Eqn. (1b) and setting m or n to 1 respectively.

A program has been written which lays a mesh on the plate and computes all the mode shapes needed to find the response of a plate up to a given maximum frequency. The frequency range of interest to us is 20 – 20,000 Hz, the range of human hearing. The mode shapes are computed and then stored in a 4D array – (n x m) x (x x y) – to allow them to be called quickly for later parts of the program, namely to find the response at any given frequency using the summation over modes given by Eqn. (2). For a maximum frequency of 20kHz, we need to perform a summation of the order of 40x40 (nxm), dependent on plate parameters. When calculating the response at high frequencies this summation is rather time consuming, but the program has been written to sum over fewer modes at low frequencies – dramatically speeding up calculations. When calculating the response at a given frequency, a unit input force is assumed, ie F = 1 in all cases.

2.1.3 Resulting Investigative Tools

Using this model for the response of a plate, three key tools were developed to aid investigation of DMLs. The first is an animation (slowed down) of the harmonic response at any frequency. This allows us to view the deformation and wave patterns of the plate. This animation is simply performed by multiplying the *complex* displacement given by the model with a rotating exponential function, and plotting only the *real* part of the resulting displacement. The second tool is also an animation but this time animates the displacement shape as we scan up in frequency. This is extremely instructive in showing us how the nature of deformation changes with frequency. To perform this animation we must re-compute the response at each frequency step, and plot the resulting *real* displacement. At all frequencies the level of displacement is rather small (<0.1 mm for 200 x 200 mm panel) so the animation displacements are scaled to give the viewer a clear idea of the mode shapes and wave patterns.

Figure 3 – Snapshot of Harmonic Animation Tool

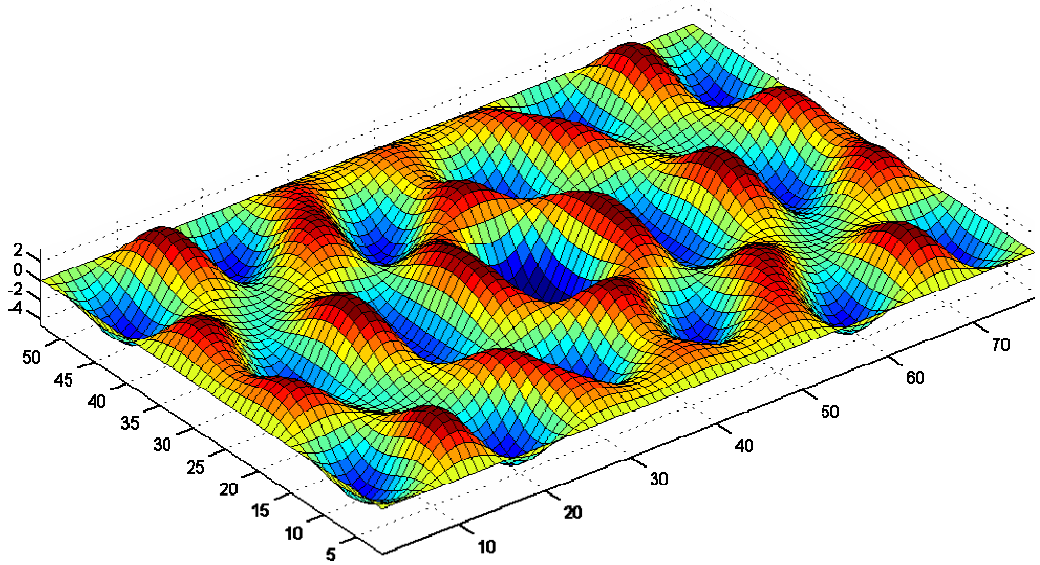

This snapshot is taken from the MatLab animation tool developed to view the response of a panel. The above response is found for a 20x12x0.1cm steel panel being excited at 2000Hz. The x and y axis describe the mesh grid position, and the z axis describes the normalised plate amplitude.

The third tool is one that computes the mobility transfer function from one point on the plate (force input) to another (velocity output). This lets us quickly visualise what the plate is doing at various frequencies, and gives an insight into some of the key parameters such as modal density and modal overlap factor. To validate the model we used the transfer function. We first computed the parameters modal density, modal overlap factor, and critical frequency. These are dependent on the plate dimensions and

materials and can be easily calculated [see Appendix 2 for equations]. These parameters are the basis for statistical element analysis (SEA) and have allowed the model to be verified as correct against SEA predictions [see Appendix 3 for one such verification]. The model and SEA predictions are in agreement and so we can trust the model output.

2.2 Coupling Panel to Surrounding Air

2.2.1 Theory

When analysing the acoustical properties of a vibrating structure, it is the power radiated as sound waves into the surrounding air that is of key interest. The Rayleigh integral describes the pressure in space as a result of a vibrating planar structure, from which we can calculate the total power radiated:

$$p(\mathbf{x}) = -\left(\frac{\rho_a \omega^2}{2\pi}\right)\iint_A \left(\frac{e^{-ik_a r}}{r}\right) w(\mathbf{x}')d\mathbf{x}', \quad r = |\mathbf{x} - \mathbf{x}'| \tag{4}$$

The pressure, p, at a location $\mathbf{x}$ in space is defined in terms of the complex displacement $w(\mathbf{x}')$, the air density ρ_a, acoustic wave number k_a, and the frequency of vibration ω. Calculating the power radiated by integrating over the volume is cumbersome and time consuming, but we can greatly simplify the problem by using the Jinc function method. We can calculate the time averaged power radiated by the plate by using the following equation:

$$P = \frac{\omega}{2} \times \mathbf{a}^{*T}\,\mathrm{Im}(\mathbf{D})\,\mathbf{a}, \qquad \mathbf{a}_n = \frac{\pi}{2} \times u(\mathbf{x}_n) \tag{5a,b}$$

where $\mathbf{a}_n$ is a generalised coordinate, calculated trivially from the displacement $u(\mathbf{x}_n)$ given in Eqn. (2) by employing a Jinc function representation. For a baffled plate the imaginary part of the dynamic stiffness matrix, $\mathbf{D}$, can be represented as:

$$\mathrm{Im}(D_{ij}) = \frac{8\pi\omega\rho_a c_a k_a^2}{k_s^4}\,\mathrm{sinc}(k_a r_{ij}), \quad r_{ij} = |\mathbf{x}_i - \mathbf{x}_j|, \quad k_s = \sqrt{2} \times \frac{\pi}{c} \tag{6a,b,c}$$

where ρ_a, c_a, k_a, c define respectively: the density of air; speed of sound in air; acoustic wave-number; and size of mesh spacing. The variable r_{ij} is the distance between two points i and j on the plate. It is as a result of the Jinc function being radially symmetric

that we can use this simple formula for calculating the dynamic stiffness matrix, and so simply calculate the radiated power. This method computes the total power radiated in the near field, by using the air pressure at every point on the plate due to surface displacements. The total power in the near field is necessarily the same as the total power in the far field, and so this method provides a quick way of computing the far field power, which is of interest when analysing the acoustical properties of DMLs.

When analysing the power radiated from a flat plate it is instructive to have some idea of the region in which it is operating. The key parameter here is the *critical frequency*, the frequency at which the acoustic wave number equals the plate bending wave number. The combination of critical frequency and excitation frequency tell us how efficiently different modes will radiate. Maximum efficiency occurs when modes are excited at their *coincidence frequency* or above (see Figure 4 below), coincidence frequency being the frequency at which bending waves 'fit' acoustic waves, ie their wave numbers match.

Figure 4 – Typical Radiation Efficiency for a Single Mode

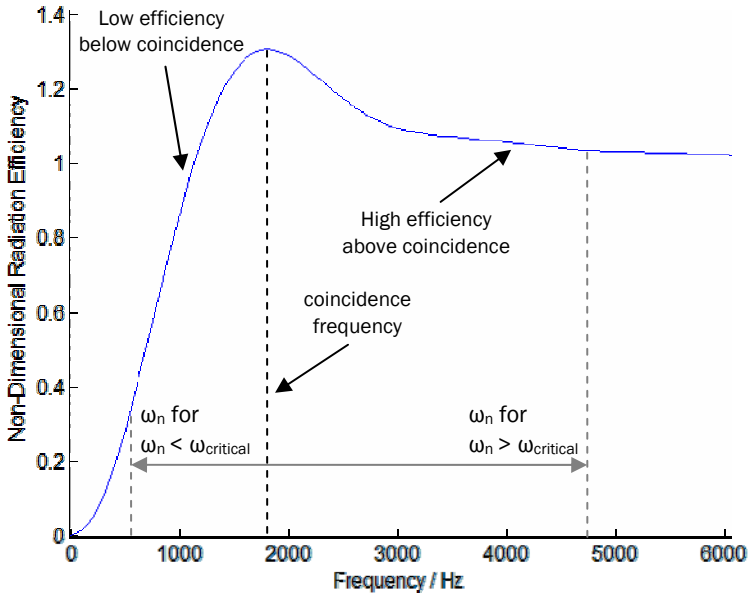

A typical mode has low radiation efficiency below its coincidence frequency. If resonance occurs below coincidence, low efficiency will occur at resonance. The mode will resonate below its coincidence if $\omega_n > \omega_{critical}$. Similarly, modes that resonate above $\omega_{critical}$ will resonate with high efficiency. The plot shown is for the first mode (1,1) of a 19cmx19cm steel plate.

If we excite a plate below the critical frequency we find that modes with high radiation efficiency resonate well below the excitation frequency and so do not have high amplitude. Resonant modes have high amplitude but low efficiency, and so no particular

modes dominate the response. If we excite the plate above the critical frequency however, we find the resonant modes have high amplitude *and* high efficiency and so will be dominant. It is this change in behaviour that makes the critical frequency of such importance to the investigation of flat plate sound radiation.

2.2.2 Modelling Technique

A program has been written in MatLab to perform the calculations defined in Eqns. (5) and (6) to find the power radiated from the plate at a given frequency. It is a testament to the simplicity of the Jinc function method that once the displacement $u(\mathbf{x_n})$ has been found using the previous model, only a few lines of codes allow us to find the power radiated. To populate the matrix $\mathbf{D}$ it was decided to find a matrix $\mathbf{R}$ such that $r_{ij} = |\mathbf{x}_i - \mathbf{x}_j|$. Originally this was performed as a double *for-loop* but this proved extremely slow. $\mathbf{R}$ has dimensions of (a x b) x (a x b), where a and b are the number of points in the mesh in the x and y directions respectively. For a mesh of 20 x 20 this leads to dim($\mathbf{R}$) = 400 x 400. The final size of $\mathbf{R}$ is proportional to the mesh resolution c to the power 4, and so not only is $\mathbf{R}$ very large, but it can increase in size very quickly for a small increase in resolution. A fast way of computing $\mathbf{R}$ was needed.

MatLab is fast at computing matrix calculations, and copes well with complex numbers, but is rather slow at for-loops. To avoid using for-loops a program to populate $\mathbf{R}$ was developed that described the x and y position of each mesh point by using real and imaginary components, and used MatLab's in-built (and highly optimised) 'abs' function to find the distance between pairs of complex points [see Appendix 4 for program code]. This neat method resulted in a speed up of over 100x when computing $\mathbf{R}$, and so allowed the power at any given frequency to be calculated in a fraction of a second. The matrix $\mathbf{R}$ was stored, meaning that after the first power calculation the power could then be calculated at other frequencies by recomputing $u(\mathbf{x_n})$ and using Eqns (5) and (6) with $\mathbf{R}$ as before.

To validate the power calculations, plots of non-dimensional frequency ($k_{non\text{-}d}$) versus non-dimensional radiation efficiency (σ) were found for the first 6 modes of vibration. $K_{non\text{-}d}$ and σ are found directly using:

$$\sigma = \frac{8\omega^2 c^4}{c_a^2 L_x L_y \pi^3} \mathbf{a}^{*T} \mathrm{sinc}(k_a \mathbf{R}) \mathbf{a}, \qquad k_{non-d} = \frac{\omega}{c_a \pi \sqrt{\frac{n^2}{L_x^2} + \frac{m^2}{L_y^2}}} \qquad \text{(7a,b)}$$

where L_x and L_y define the plate dimensions in both planar directions, and all other symbols are as described previously. We can see that σ is directly proportional to the power calculated using Eqns. (5) and (6) and so if we calculate σ using the same steps as we do the power then σ is a suitable variable to validate our coupled model. Plots of σ vs $k_{non\text{-}d}$ were performed for a square steel plate and the results validated against benchmark results found using the FFT method [Williams & Maynard, 1982]. The model and benchmark results show excellent agreement and so we can take the model as predicting the radiated power accurately [see Appendix 5 for graph].

2.2.3 Tools Developed

Using the air-coupled model of a DML, two key tools were developed to aid investigation of these speakers. The first is a program that computes and plots the power transfer function, found by calculating the radiated acoustic power at a series of frequencies. This allows us to see what kind of acoustical response different DMLs have, ie smooth and flat (this is desirable for loudspeakers) or modal and jagged. Initially a strange phenomenon was observed – at a high frequency the transfer function would suddenly rise in amplitude. The reason for this is not due to the physics of the plate, but is in fact due to a breakdown in the Jinc function method. This occurs when the mesh grid being used over the plate is of too large a spacing to describe high wave numbers.

Figure 5 – Breakdown of Jinc Function Method at High Frequencies

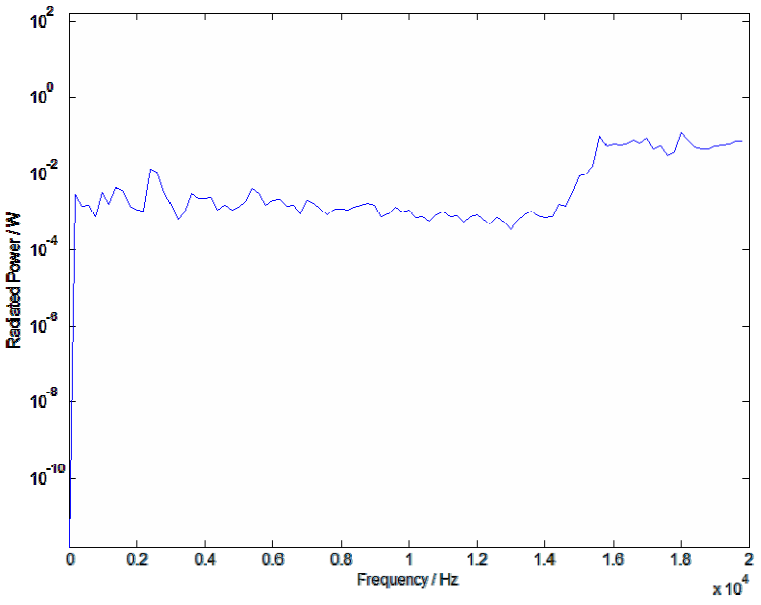

The Jinc function method breakdown is seen as a large rise in predicted radiated power at 14kHz. This breakdown occurs when the wavelength of resonant modes is shorter than half the grid spacing of the wavelet mesh used to describe the plate.

The Jinc wavelets can only be used to describe bending waves that have a half wavelength larger than grid spacing of the mesh. A conservative value for the maximum frequency of bending waves that can be depicted using the mesh is given by:

$$\omega_{\max} = \left(\frac{D}{\rho h}\right)^{1/2} \times \left(\frac{\pi}{c}\right)^{2} \tag{8}$$

For the plate used to compute the power spectrum shown in Figure 5 above, this maximum frequency turns out to be ω_{max} = 14kHz, above which the spectrum goes awry. A simple check was added to the program to stop the spectrum being computed above this breakdown frequency, ensuring accurate (but sometimes truncated) results. This model takes anywhere from a few minutes to a few hours to produce a 4000 point power spectrum. The variation in time is as a result of the number of mesh points. Even when taking a few hours this is far faster than FEA or BEM computations. The speed of computation allows for many models to be run in order to fully analyse the effect of different parameters on the power spectrum.

The second tool is one that computes the non-dimensional radiation efficiency for each mode, and then plots this as a surface in the modal domain (ie plots $\sigma_{n,m}$ at (n,m) for all modes used within our model). This allows us to see how close each mode is to resonating at maximum efficiency, ie when $\omega_{res} = \omega_{coincidence}$. By visualising this we see which region of operation the plate will be in at low and high frequencies, ie is ω_{res} greater or less than $\omega_{critical}$, with the repercussions resulting from being in either region discussed in section 2.2.1. We can use this tool to understand the mode of operation of DMLs. This tool typically takes around 15minutes to run, dependent on the number of modes used within the model and so allows for quick analysis of many different panels.

2.3 Optimisations

2.3.1 General Optimisation Methods

To ensure that the models developed were of practical use when investigating DMLs, the models needed to be fast. Conventional computational methods such as FEM or BEM can take days or even weeks of continuous calculation, we needed to do this in minutes or hours. Various common MatLab optimisation techniques were used to speed up the code. These included:

1. Vectorising equations where possible to avoid the use of for-loops.

2. When for-loops were necessary, rewriting functions in-line to avoid the overhead of calling these functions
3. Splitting in-built functions into sections that must be included within for-loops, and sections that can be performed out with the loop, to avoid unnecessary re-computation
4. Using an optimised package of exponential based functions (exp, sine, sinc etc). These improve upon MatLab's inbuilt functions by not being so general purpose – they are optimised for 'double' type data only.

These optimisations saw a marked improvement in the speed of the programs, the total time needed to compute a power transfer function was decreased by 10x.

2.3.2 Outstanding Problems

There are two outstanding problems with the code in terms of how well optimised it is. The first is that it can require a large amount of RAM. This is as a result of the size of $\mathbf{R}$, which is regularly over 250MB in size. Thus, for Eqns. (5) and (6) we need approximately 4x250MB = 1GB of free RAM to allow the power prediction program to run completely within memory, which is critical to ensuring fast computation. Few desktop computers have enough free RAM to run these programs in this manner, and so a server was used that contained 6GB, thankfully more than enough for the plates investigated.

The other outstanding problem is that MatLab's sinc function is not very fast and is the bottleneck in computing Eqns. (5) and (6). This has been improved by optimising in the manner discussed in the previous section but even after re-writing sinc inline and using an optimised sine function, computing sine($k_a\mathbf{R}$) takes 75% of the time of the whole program. This is clearly the first point of call if the program needs to be optimised further, though the author has reached the limits of his optimising tricks.

Section 3: Investigating the Loudspeaker

3.1 Finding Loudspeaker Panel Parameters

3.1.1 Dismantling the Speakers

To investigate DMLs it was necessary to determine the parameters of some real speakers to feed into the model. A pair of second hand Packard Bell FSP-100 DMLs were sourced and carefully taken apart [see Figure 6 below]. Each speaker is comprised of:

1. A stiff plastic panel, with fake dust cover on front side
2. A rigid steel frame, with concave perforated back plate
3. Electrically driven magnetic voice coil, positioned centrally

The plastic panel is a section of two-ply corrugated polypropylene board, corrugations running lengthways along the panel. This suggests that the panel will not have uniform stiffness, as assumed in the model so far. The panel is simply glued around its outer edge into the frame.

Figure 6 – The Specimen DML

A Packard Bell FSP-100 flat panel PC speaker. Dimensions approximately 20x12cm. Pen shown for reference.

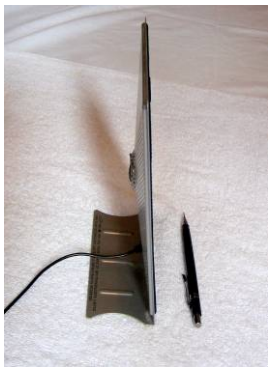

The thickness of the speaker reaches a maximum of 15mm in centre of concave back plate.

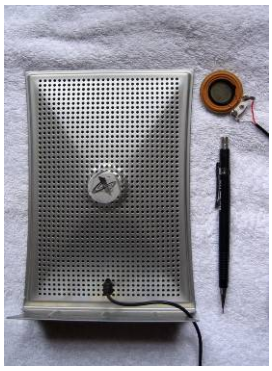

Perforated concave metal back plate. Voice coil shown to top right. Voice coil sits in circular recess in centre of back plate

Corrugated plastic panel. Circular mark seen in centre due to voice coil. Soft synthetic cloth dust cover covers front side of panel and is glued tight on back as shown.

The panel was prised out of the frame using a flat blunt knife, and care was taken to avoid deforming either the panel or frame in the process. The mass of the steel frame is sufficiently large compared with that of the panel that we can assume it is rigid in space during operation. Also, the glue that holds the panel in place is not very strong, and is

only applied on the outer few mm of the panel, so our assumption of a simply supported boundary condition seems plausible. One should note however that the weak glue will likely be dissipative and result in a large degree of boundary damping. The panel was measured and the resulting parameters are shown in Table 1 below:

Table 1 – Specimen Panel Parameters

Parameter	Symbol	Value
Length	L_x	187 mm
Width	L_y	~128 mm *
Excitation Point	(x_o, y_o)	(93,64) mm
Thickness	h	4 mm
Mass	M	18.25 g
(Density)	(ρ)	(194 kg/m3)

* The panel has long edges that are slightly concave – width varies between 121mm in centre and 131mm at top and bottom

The density ρ was assumed to be uniform and calculated using the other measured parameters. The point of excitation was found to be in the very centre of the panel.

3.1.2 Stiffness Test

A key parameter needed in the model is that of D, the bending stiffness. This was found by performing a standard bending stiffness test – applying a load and measuring the resulting deflection [see Figure 7 below]. This was performed in both directions, x and y, to find the variation in stiffness between the two directions due to the plastic corrugated ribs. Care was taken to apply an even load across the free end by using a rigid brass plate to allow the panel to be treated as a beam. Deflection measurements were taken quickly to avoid errors due to a small amount of plastic deformation that was observed.

Figure 7 – Images of Panel Stiffness Test

Brass plate placed at edge of panel to ensure even spread of load. Load applied at midpoint of panel edge. An evenly spread load avoids any torque and allows bending beam equation to be used.

Load applied at edge of panel and resulting displacement measured in vertical direction. Measurement taken quickly to avoid plastic deformation.

If the load is applied evenly and the panel treated like a beam, we can use the equation for a clamped beam:

$$D_x L_y = EI = \frac{W l_x^3}{3\delta} \tag{9}$$

where W is the applied load, δ the resulting deflection, and l_x the length of the free section of the panel. Similarly this equation can be applied in the y direction. By plotting δ against W and taking the gradient we can then gain an estimate for the bending stiffness D. Plots in both directions are shown below in Figure 8; as expected the relationship is remarkably linear.

Figure 8 – Results From Stiffness Test – Deflection vs Load

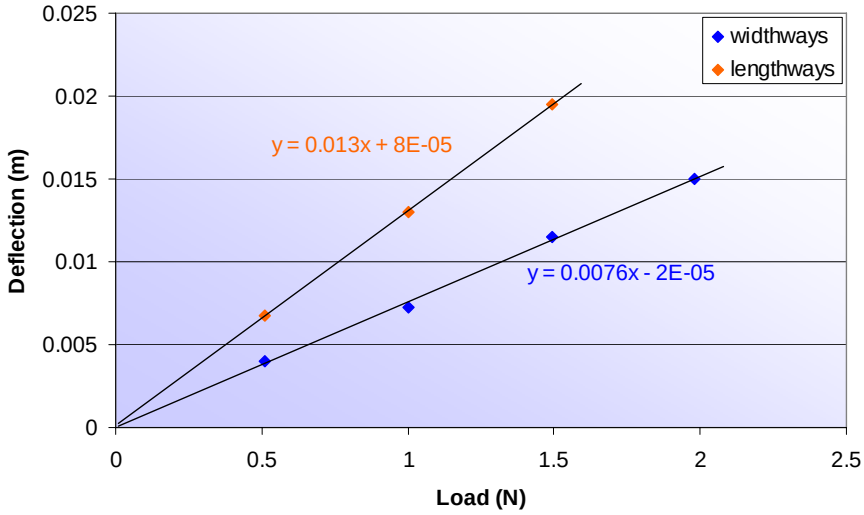

A linear relationship is seen in both planar directions. Lines of best fit and equations are shown above. The predicted y axis intercept approaches zero for both cases, and so we can assume that stiffness is also linear at smaller deflections than the range measured experimentally.

The deflections measured are far greater than those experienced during normal operation of the DMLs, but the plots are linear enough that we can assume the stiffness calculated here will be the same for small deflections. The results in both directions are shown below:

Table 2 – Panel Stiffness Values

Direction	Stiffness Symbol	Value (Nm)
Lengthways	D_x	0.80
Widthways	D_y	0.22
Average	D	0.51

As expected the stiffness is different in each direction, though in the same order of magnitude. To simplify future analysis we assume that the stiffness D is uniform, and has a value that is the mean of the values found experimentally.

3.1.3 Laser Vibrometer Testing

The final parameter that is needed to run the model is the damping coeffiecient, η, of the panel. To find the damping of a vibrating structure it is common to excite the structure and perform modal analysis on the resulting transfer function. The panel is extremely light and so attaching even a small accelerometer will result in too large a

change in mass for accurate results. With this in mind, a laser vibrometer was used to measure the surface response due to excitation, in this case performed by a short tap from an impulse hammer. The hammer tap was applied at the same point in the panel's centre that the electromagnetic voice coil had been attached, to try and excite the same modes in testing as in normal use.

Figure 9 – Laser Vibrometer Testing

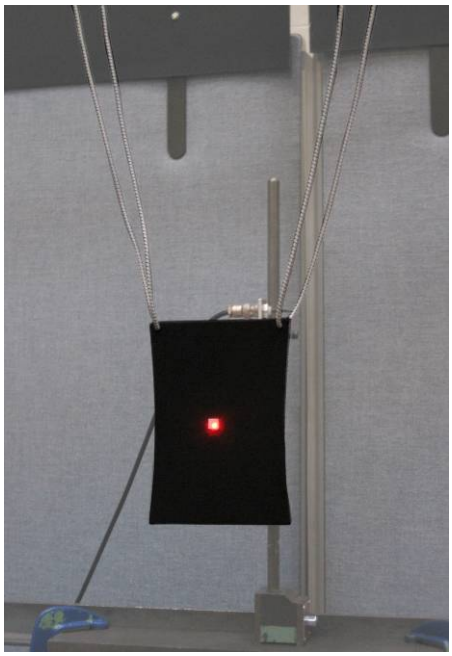

Panel suspended by elastic chord through top corners. Laser aimed at reflective sticker placed in centre of panel.

Impact hammer used for test, released to swing under gravity to give impulse. Tip of medium hardness used.

The laser vibrometer measured the response of the central point – ie a driving point response. The model predicted and experimental mobility transfer functions agree well for low frequencies [see Appendix 6]. All predicted modes within the model are shown experimentally, with small differences in resonant frequency being due to the different edge conditions imposed upon the panel for each method. Some extra modes are found experimentally that are not shown in the model spectrum. Some of these are anti-symmetric modes that occur because the impact did not occur *exactly* on the centre of the plate, and so were excited experimentally but not within the model. The few remaining unaccounted modes are due to resonances of the whole system, ie the system of the panel and the elastic suspension ropes. At frequencies above 1khz the experimental spectrum becomes less clear and unsuitable for modal analysis.

We can use the low frequency region to find the damping of the panel. This was performed by looking at the sonogram of the first few seconds after impact and calculating the damping at a range of frequencies by using the exponential decay of each. The damping decreases with increasing frequency, to an asymptote of approximately 0.014 [see Appendix 7 for detail]. It is thought that the high damping at low frequencies is predominantly due to boundary damping (longer wavelengths are affected by boundaries more strongly), and that at high frequencies the internal damping of the panel dominates. In this experimental case the boundary damping is due to friction and small impacts of the elastic cord in each corner hole. When the panel is in the speaker frame the boundary damping will be caused by the glue holding it in place along its edge. This is very tacky and will be highly dissipative, greatly increasing the damping at low frequencies. The internal damping that dominates at high frequencies is high for a plastic panel (0.014). This was thought to be due to the fake dust cover on the surface of the plastic panel. The soft fabric is pulled tightly over the front of the panel – a crude damping treatment as well as an aesthetic addition.

The model uses a constant damping value, and this was assumed to be the mean of the damping values recorded experimentally – μ = 0.05, but in reality the panel will have higher damping at low frequencies (due to glue on edges) and lower damping at high frequencies (internal damping).

3.1.4 Modal Parameters

Some parameters that give us an insight into how the panel is operating are those used within SEA, specifically modal density, n_d, critical frequency, ω_c and modal overlap factor, m_d. For a flat plate these can all be calculated directly [see Appendix 2]. Using the dimensions and material values found for the real panel, these modal parameters were found, see Table 3 below.

Table 3 – Modal Parameters for Experimental Panel

Parameter Name	Symbol	Value
Modal Density	n_d	0.0152 modes/Hz
Critical Frequency	ω_c	23.1kHz
Modal Overlap Factor	m_d	7.61 @ 10kHz

The panel has a very high critical frequency, slightly above that of the operating region of loud speakers. These means that all modes will be operating below coincidence, though

at high frequencies some modes will be approaching coincidence. The modal density is high, with approximately one mode every 65Hz. This results in a high value for the modal overlap factor: we expect to see a smooth transfer function especially at high frequencies. It should be noted however that due to the driving point being positioned in the centre of the panel anti-symmetric modes will not be excited and so the modal density in practise will be half that calculated here.

3.2 Model Results

3.2.1 Radiation Efficiency Plot

As found in section 3.1.4 the panel operates with all modes below coincidence. To see exactly how close to coincidence each mode operates, the tool that computes a plot of non-dimension radiation efficiency for each mode was used. The resulting image is shown below:

Figure 10 – Radiation Efficiency of Modes of Experimental Panel

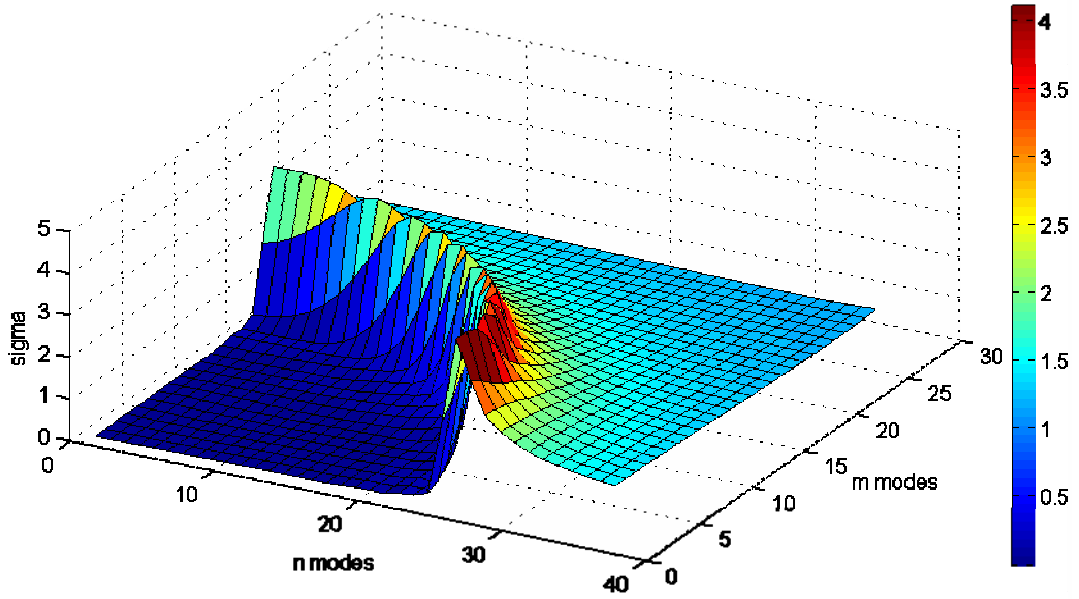

The above surface plots shows a ridge at 23kHz, where modes resonate at their coincidence frequency. All modes below 20kHz are shown in the dark blue region, resonating well below coincidence. Modes at 20kHz are found on the n axis at (24,1), and m axis at (1,16).

This plot shows the radiation efficiency $\sigma_{n,m}$ for all modes used within the model (ie $1.5n(max)$ x $1.5m(max)$), and thus shows many modes that are above coincidence. These modes, however, resonate well above 20kHz and so will not contribute much to the overall response. The important point to note from the plot is that the transition to coincidence at 23kHz is very steep, and so all modes below 20kHz have a comparable

low radiation efficiency value. Thus, there should be a fairly even value of radiated power across a large frequency range, with all resonant modes radiating at a similar efficiency below coincidence. This would not have been the case had the critical frequency been below 20kHz. We also see from the plot the high modal density, with approx 300 modes below coincidence at 23kHz. Again this will result in a smooth power spectrum, as resonances merge into one another.

3.2.2 Complete Power Spectrum

The key result for analysing the method of operation of vibrating panels is the power spectrum for radiated power. Using the tools developed previously this was computed for the real panel parameter values found in section 3.1. The resulting spectrum is shown below:

Figure 11 – Modelled Power Spectrum of Experimental Panel

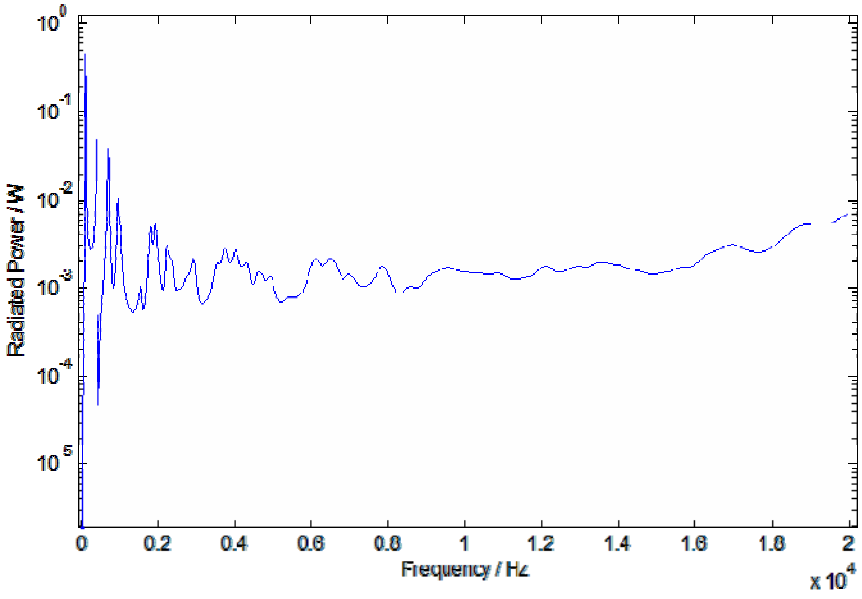

Model predicted power spectrum for experimental panel. After an initial low frequency modal region the spectrum is remarkably flat.

The key features of this spectrum are:

1. Distinct modes below 1kHz
2. A very flat response above 3kHz, almost horizontal at 10kHz
3. A gentle rise in radiated power at high frequencies

The first feature is to be expected, as at low frequencies the modal overlap factor is very low giving rise to distinct modes. The last of these features can be explained by looking

at radiation efficiencies in Figure 10 above. At high frequencies our modal summation will include some modes that are approaching coincidence, and so the overall radiated power will increase. What is interesting here is quite how flat the spectrum becomes at 10kHz.

3.3 Explaining the Radiation Method

3.3.1 Infinite Plate Theory

One possible mode of operation of the panel is that it has such high damping that it radiates much like an infinite plate. For an infinite plate (or finite plate with extremely high damping) the waves that are created by the excitation point decay quickly and do not interact with a boundary. The resulting wave pattern is of all waves travelling outwards like ripples in a pond. In this scenario all sound power will be radiated from the driving point, which will act as a point source. If the DML operates as a point source it explains why we do not see any beaming for this type of speakers.

For an infinite plate radiating below its critical frequency, the power radiated from the driving point can be calculated directly [Fahy, 1987 p94]:

$$P_{\inf} = \frac{\rho_a F^2}{4\pi c_a (\rho h)^2} \tag{10}$$

where F is the force of excitation (assumed to be 1 for all calculations). This value was calculated using the experimental panel material properties, and was compared with the model predicted power:

Figure 12 – Power Spectrum and Infinite Plate Radiation

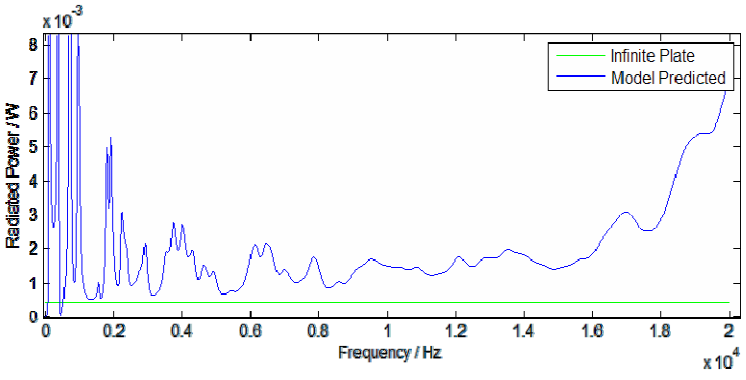

The power radiated from an infinite plate is constant at all frequencies, radiating from the driving point like a point source. The power from an infinite plate with the same properties as the experimental panel is lower than that of the panel but in the same order of magnitude.

Though the power from an infinite plate is of a similar magnitude to that of the model, the model is approximately 3x greater. Some other method of radiation is occurring, but of comparable magnitude to that of an infinite plate.

3.3.2 Effect of Changing Damping

Previous results showed that the panel radiates power of a level comparable to that of an infinite plate. It was questioned as to exactly how close the behaviour of the panel was to that of an infinite plate. An infinite plate can be realised in practise by using a finite plate with extremely high damping. With this in mind, the damping of the model panel was varied from 0.25% to 50% and the radiated power calculated using the power spectrum tool. The mean power in the region 7.5 – 17.5kHz (the 'flat' region) was calculated for each panel and plotted against damping.

Figure 13 – Power vs Damping for Experimental Panel

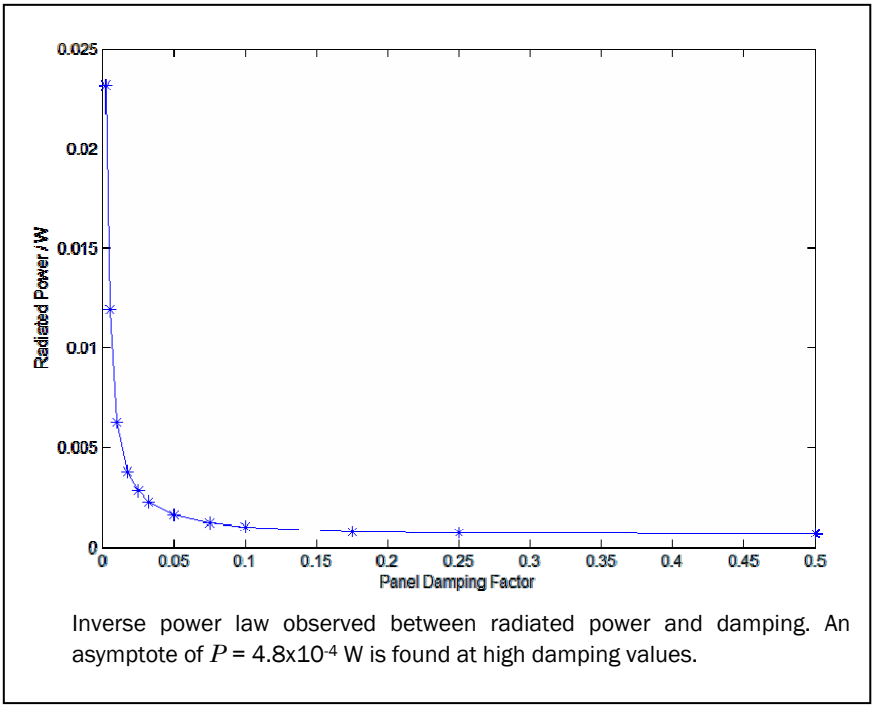

Inverse power law observed between radiated power and damping. An asymptote of P = 4.8x10^{-4} W is found at high damping values.

At high damping values the radiated power tends to a limit. The relationship of radiated power to damping was modelled as an inverse power law plus a constant offset, and using a curve fitting tool this offset was found to be 4.8x10^{-4} W. This agrees favourably with the infinite plate value found using Eqn. 10, P_{inf} = 4.6x10^{-4} W. The graph shows us that the damping value of 0.05 used within the model of the real plate puts us in a region that is quite close to exhibiting infinite plate behaviour in terms of the power

radiated. It was thought that the radiation from the driving point must account for at least some of panel radiation.

By using the animation tool we find that the real panel is vibrating in a rather special manner in the flat region:

Figure 14 – Experimental Panel Response at 10kHz

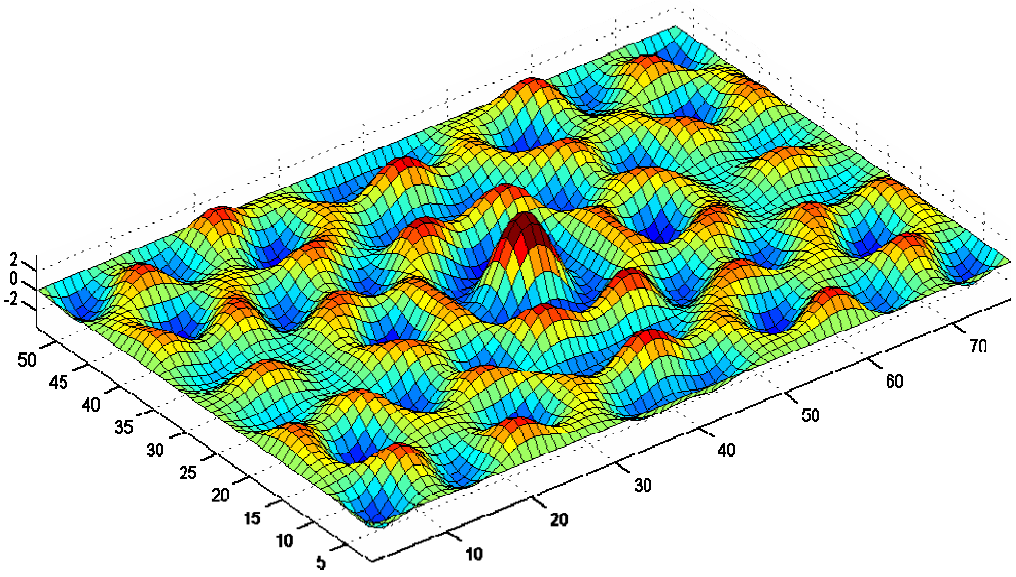

The panel exhibits infinite plate behaviour (large response at driving point) and also reverberant behaviour (semi-random wave pattern in surrounding region).

Thin plates usually vibrate in one of two distinct manners: if damping is high then the response is like an infinite plate, or if damping is low then the waves reflect off edges to create a semi-random reverberant field. The reverberant field consists of multiple uncorrelated modes superimposed on one another. The direct field experienced in an infinite plate can be thought of as consisting of multiple modes with high correlation – ie all tracking the central driving point. The model panel exhibits *both* types of behaviour: the driving point being much higher in amplitude than the surrounding displacements, but the surrounding displacements being semi-random and all of similar amplitude. Does the reverberant field radiation account for the difference between our model predicted radiation and that of an infinite plate?

3.3.3 Accounting for Reverberant Field

To analyse the power radiated by the reverberant field a method for calculating it was needed. The reverberant field radiation at any frequency can in fact be calculated directly using an SEA approximation [Lyon R, 1975, p234]:

$$P_{rev} = \omega \eta_{rad} E_p \tag{11}$$

where P_{rev} defines the acoustic power radiated due to the reverberant field, η_{rad} the radiation loss factor resulting from coupling the panel with the surrounding air, and E_p the energy within the vibrating plate. The energy can be eliminated by noticing that a similar SEA equation holds for the power input to the plate at the drive point:

$$P_{in} = \omega \eta E_p \qquad \Rightarrow \qquad P_{rev} = \frac{\eta_{rad}}{\eta} P_{in} \tag{12a,b}$$

where η refers to the plate loss factor, or *damping*, as before. We can calculate the input power directly [Lyon R, 1975, p49]:

$$P_{in} = \frac{\pi n_d}{4 \rho L_x L_y h} \tag{13}$$

To find the radiation loss factor η_{rad} we find there is a direct formula for baffled plates [Fahy 1987 p237]:

$$\eta_{rad} = \frac{\rho_a c_a L_x L_y \sigma}{\omega M} \tag{14}$$

where σ defines the radiation efficiency as before. Having computed σ at resonance for all the modes of interest in our model (section 3.2.1) this data was used to estimate σ at a given frequency of interest, allowing η_{rad} to be calculated and so P_{rev} found.

The radiation efficiency was estimated by taking an average efficiency of those modes with resonant frequencies close to the given frequency of excitation, ω. Only modes close to the frequency of excitation will respond strongly, and they will all have a similar radiation efficiency (as shown by Figure 10 above). Thus, it was thought to be a satisfactory assumption to take the mean efficiency of these modes when calculating σ. Modes 'close' to the frequency of excitation were defined as having resonant frequencies within $\omega \pm 10\%$. This was felt to be a reasonable approximation for the region of modes that would contribute towards the displacement of the panel. Using this approximate value for σ at each frequency a power transfer function for P_{rev} was found, as shown in Figure 15 below:

Figure 15 – Model Predicted and Theoretical Power for Experimental Panel

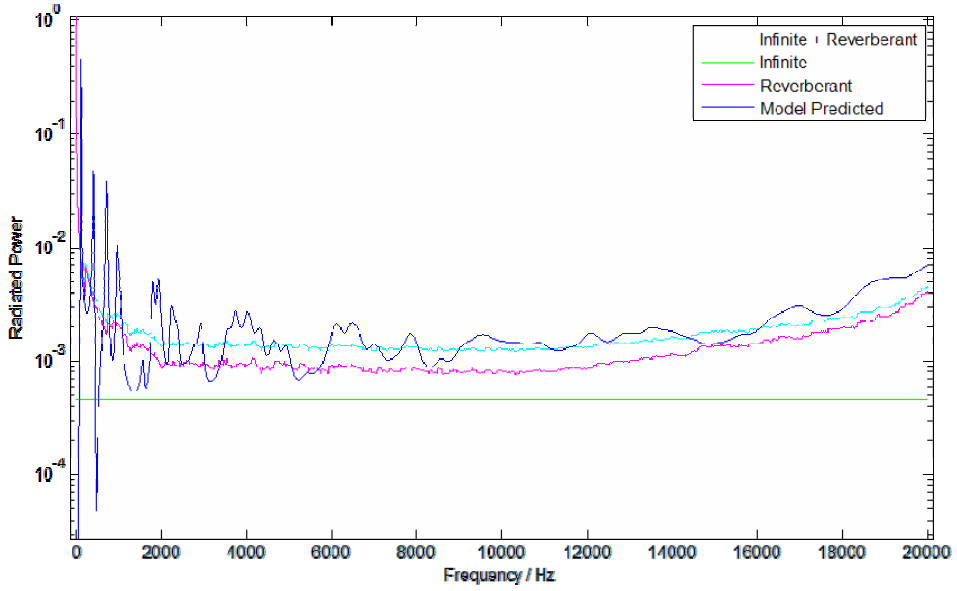

By adding together theoretical values for infinite plate and reverberant field behaviour excellent agreement with model predict results is seen.

The power radiated due to the reverberant field is slightly too low to account for all the power from the panel, but when the driving point radiation is added the combined power is strikingly similar to that predicted by the model. The theoretical combined power is smooth (save for some noise due to using a discrete sample of modes) and does not show the detail of the model prediction, but shows the same general trend. The lack of detail is due to using an SEA approximation when calculating the radiation from the reverberant field. The agreement between this theoretical spectrum and that predicted by the model validates the theory that the panel operates with both driving point and reverberant field radiation being significant to the total power output, as noted when looking at the displacement pattern (see Figure 14). The combined theoretical power is slightly lower than the model predicted power at high frequencies. The model is thought to be correct and so the theoretical value is under-predicting at high frequencies. This is due to the region of modes used to find σ at high frequencies. Modes slightly higher than this region will not have a large amplitude but will be at coincidence or above and so will be radiating extremely efficiently. If the region used is increased from $\pm$ 10% to $\pm$ 15% we include these efficient modes in our calculation of σ and see a much better agreement between the model predicted and theoretical radiated power. However, if the region is increased much further then the theoretical value *over* predicts at high frequencies. The correct region to use when calculating σ depends on critical frequency

and modal density, and will vary from plate to plate, hence choosing this region is somewhat of an art.

3.3.4 Applying Dual Radiation Theory to Alternate Panels

It has been shown that for the DML analysed the acoustic radiation can be split up into two distinct radiation methods that can be easily computed using an SEA approximation. To validate the theory that these two methods occur somewhat independently and sum to give the total power, the theoretical result was plotted against the model predictions for some other panels. The two very different panels were modelled – one small stiff panel (where the radiation from the reverberant field dominates total radiation), and one large less stiff panel (where the driving point radiation dominates). For both cases we see excellent agreement between theoretical radiated power and model predicted power [see Appendix 8 for plots]. It is important to note that we have modelled one panel with 1/4 of the area of the original, and one panel with 1/10 of the stiffness of the original, yet both panels still have a significant contribution from *both* types of radiation, as was found for the original panel. It is thought that this dual radiation method is found for panels of a wide range of parameter values, and so one can surmise that this is the radiation method operating in all DMLs.

3.3.5 Computational Use of Dual Radiation Method

The dual radiation method for calculating the radiated power from DMLs uses a computationally trivial direct calculation if σ is known. This SEA approximation of the power spectrum shows none of the detail of the power spectrum predicted by the full model. However, as the full model shows, DMLs quickly have a high modal overlap factor as the frequency increases, and so settle down to give a very flat response. The response is so flat that above the initial modal low frequency region the direct method for calculating the power is typically within 3dB of the model predicted value. It should be noted that the extremely high edge damping experienced by the panel when glued into the speaker frame has not been included in the model. The low frequency region is expected to have higher modal overlap than predicted by the model and so the initial modal region will be contained to lower frequencies. Many DMLs are rated as operating from 300Hz – 20kHz, and so it is expected that the edge damping lowers the modal region to be confined to below 300Hz. Thus, the dual radiation method will show a good approximation to the model for all frequencies above 300Hz, ie the working range of the

speaker. This means that the approximate power response for the full working range of a DML can be calculated in 15mins; 15mins to calculate σ for each mode, and negligible time to compute P_{tot} from σ. This is an extremely useful tool when designing and analysing such speakers.

To speed up the computation still further a fast method of computing the radiation efficiency is needed. There is one such direct method for finding the average radiation efficiency that is extremely fast to compute [Leppington et al, 1982]. This has the added benefit of computing the *average* radiation efficiency, ie we do not need to guess a suitable region of modes over which to average σ. This method will allow the power spectrum for a flat panel to be computed in a fraction of a second.

3.4 Analysis of Theory

3.4.1 Desirable Properties of DML

For accurate sound reproduction we require loud speakers to have a flat radiated power spectrum. Through analysing a real DML using the computational model developed in this research it has been found that the acoustic response of this DML is indeed very flat over a large range of frequencies. As discussed above, the modal low frequency region will likely be confined to an even lower frequency when the panel is sitting in the frame, and a relatively flat response will be seen from 300Hz – 20kHz. The power that radiates from the drive point contributes to the flat response by being constant at all frequencies, but also has the desirable property of radiating power evenly in all directions, as if it were a monopole. The power radiated due to the reverberant field is also thought to be highly dispersed. A single mode will radiate sound with some directivity, and will have a specific radiation pattern. The high modal density of the DML ensures that many modes are active, each with a different radiation pattern. When these patterns are added together the resulting radiation pattern is thought to be averaged over space, and so will not have a high directivity. The modal density of the plate is constant with frequency and so it is not expected that the degree of directivity will vary much once into the working region of the speaker. This is highly desirable when trying to fill a space with even sound, and is the main improvement over 'beaming' conventional speakers.

The one undesirable property of DMLs is the relatively high value of 300Hz for the start of the working region. This is dependent on the fundamental wavelength and damping of the panel. For the Packard Bell speakers analysed here the fundamental

mode is at 110Hz. To reach as low as 20Hz we would need an extremely large plate, and so most manufacturers choose to use DMLs in conjunction with a separate (piston-cone) subwoofer.

3.4.2 Comparison with Conventional Loud Speakers

It is interesting to compare the efficiency of DMLs and normal piston-cone loud speakers. For conventional loudspeakers the efficiency is rather difficult to estimate. Often efficiency is defined by a sensitivity rating, the sound level (ie acoustic intensity) at 1m from the speaker when a 1W input is given. This is typically of the order of 90dB for conventional loudspeakers. Using the model predicted power for the Packard Bell DMLs analysed, we see that the locally averaged acoustic power is never less than $1.2\text{x}10^{-3}$ W. This power is as a result of P_{in} = 0.1W, found by Eqn. 13. It was assumed that the magnetic voice coil driving the panel has an efficiency of 20%, and so the total electrical power in to the speaker was calculated as being 0.5W. The efficiency of the panel and voice coil were assumed to be constant over the working range, and so the total radiated power from a 1W electrical input was found to be $1.2\text{x}10^{-3}/0.5 = 2.4\text{x}10^{-3}$W. For DMLs the radiated sound is extremely dispersed, and so we assume that it radiates equally in all directions, giving an intensity of 83dB at 1m from the panel. This compares well with rated specifications of commercial DMLs, which are typically 85dB [Wharfedale, n.d.].

The fact that conventional speakers typically have a slightly higher sensitivity rating (90dB vs 85dB) should not be mistaken for thinking that they are more efficient. DMLs project evenly over an entire sphere, but convention loud speakers project in a wide cone shape. The sensitivity rating of a conventional speaker is taken in the middle of this cone, where the intensity is highest. If we assume that a conventional speaker projects acoustic power evenly over a cone of 90°, we find that the projection area at 1m is 0.15x that of the whole sphere at 1m. To convert the intensity of the DML to be comparable with the sensitivity of a conventional speaker we must normalise by dividing by this factor, giving a normalised DML sensitivity of 83+8 = 91dB. Rather large assumptions have been made in calculating the normalised sensitivity of the DML, but we can at least see that the efficiency of flat panel and conventional speakers is of the same order of magnitude.

The key difference between DMLs and conventional speakers is their directivity or lack of it. This difference is seen most obviously in the current uses of DMLs – in

environments where an even sound level is required: hospital p.a. systems, home cinema, car cabins. Conventional loud speakers are still typically used for high end music stereos, dj monitor speakers, and any environment where having a directed sound field and a resulting 'sweet' spot is desirable. Using the previous rough calculation for sensitivity it is interesting to note that there has not been a rapid uptake of DMLs for portable audio devices which we might expect due to their slender dimensions. Portable devices have a finite supply of power (the batteries) and so must be efficient. Though DMLs are of comparable efficiency to conventional speakers, the fact that they are not directed means that the sound intensity for a given power input is lower than that in the centre of projection of a conventional speaker. Portable devices are typically used by only a few people, and are of low volume so reflections do not dominate the sound levels, it is the direct field that is key here. If the projection angle of a conventional speaker is sufficiently large to include these few listeners it will be more efficient to use a conventional speaker than a DML, with the same resultant intensity for the listeners. There are some fantastic benefits to using flat panel speakers, but not in every situation.

Section 4: Conclusions

4.1 Novel Modelling Method

A novel method based on Jinc function wavelets has been employed to calculate the power radiated from a DML. This method improves upon FEA and BEM by taking far less time to compute, especially at high frequencies. It is thought that this is one of the first uses of this new method, and the first time DMLs have been modelled in this way. The method has been shown to be a powerful tool in practical vibro-acoustic problems.

4.2 Findings

4.2.1 Panel Radiation Method

The key finding of this research is that the sound emitted from a small DML is due to two wave-field phenomena – point source radiation emanating from the central driving point, and scattered radiation from a reverberant bending wave field. The two methods of radiation are of similar magnitude, and both have a dispersed radiation pattern. This research has resulted in the full analyse of one specific DML, but by simulating other panels it has been shown that the dual radiation theory of sound production holds for many panels of varying dimensions. It is thought that the dual radiation theory developed for this particular DML can be applied to a wide range of DMLs, possibly all.

NXT have previously provided a brief explanation for how DMLs can radiate power in such a dispersed manner. The explanation involves the idea of a chaotic bending wave field resulting in uncorrelated sound being projected in all directions. There is a semblance of truth in their description, though it is overplayed. The chaotic wave field mentioned is simply a reverberant field, a result of using panels with high modal density. By using a panel with high damping the driving point also contributes significantly to the radiated power, though this is not mentioned by NXT. The author suspects that 'high damping' elicits less of a buzz in trade magazines than 'chaos theory'.

4.2.2 Design Parameters

The key parameters that define the response of the panel are the SEA parameters, namely: modal density and critical frequency. The experimental panel analysed was shown to have high modal density (1 mode every 65Hz), and a critical frequency above the working region (23kHz). This value of the critical frequency results in resonant

modes being below coincidence, and so no single mode dominates the acoustic response. This multimodal radiation results in a dispersed radiation pattern. The high modal density is important for two reasons – 1) it ensures the reverberant field includes many modes and so produces a dispersed radiation pattern, and 2) it results in a high modal overlap factor, giving the flat response that is so critical to the performance of any loud speaker. Now that the method of radiation is understood these parameters can be used as a design tool, optimising parameters with reference to some desired value of critical frequency and modal density.

4.2.3 Dual Radiation Method of Computation

A fast method for calculating the power spectrum for a DML has been developed. This method uses an SEA approximation for the power emitted from a reverberant field and a direct calculation for the power from an infinite plate. By accepting the dual radiation theory, we can compute an approximate result for a DML's power spectrum in minutes. This approximate result shows the general trend of the power spectrum but not the detail. The real power spectrum is so smooth at all medium and high frequencies, however, that this approximate result is typically within 3dB of the real value, even tracking the rise in power seen at high frequencies.

In this research a method was used that allowed a 4000 point power spectrum to be computed in 15 minutes. Another method is known that uses a direct calculation for radiation efficiency at resonance [Leppington et al, 1982], and will allow an approximation for the radiated power of a flat panel to be computed in seconds. For many design situations the value of being able to compute the approximate spectrum in seconds will far outweigh the value of having a precise spectrum .

4.2.4 Comparison with Conventional Loud Speakers

DMLs improve upon conventional speakers by their size and lack of directivity, and are ideal for filling a space with uniform sound. They do not improve upon conventional speakers in terms of efficiency, and so are better suited to home cinema and p.a. systems than portable audio – despite their small size. DMLs can only reproduce sound as low as their fundamental frequency, for small panels this is approximately 100Hz. Unless extremely large panels are used DMLs are generally paired with a conventional piston cone subwoofer.

Section 5: Future Work

5.1 Improving Model Accuracy

The model of a DML that has been developed through the course of this research is very general and leaves us with much scope for future work. The model used made simplifying assumptions about plate damping, stiffness and boundary conditions. Future work could involve developing a more accurate model by using a non-uniform bending stiffness value, non-constant damping value, and different boundary conditions to compute mode shapes. Finding an accurate model for damping is non-trivial, especially when the panel has peculiar boundary conditions (tacky glue). The resulting mode shapes can be used to compute the radiated power without any changes to the power spectrum tool.

Further accuracy can be gained by altering the power spectrum tool to compute the power radiated for an un-baffled panel. The method for calculating the power spectrum for an un-baffled or even partially baffled plate is known [Langley, 2007], but will require a new power spectrum computer program. This program takes the same inputs as the power program used in this research (namely the mode shape at a given frequency) and so can be used as a direct replacement of the power spectrum tool used here for a baffled plate.

5.2 Additions to the Model

Theories about the possible radiation pattern emitted from a DML have been guessed, with reference to the two modes of radiation found to be dominant. It would be useful however to compute this radiation pattern directly and visualise it in 3D space. This can be done using either the Rayleigh Integral (slow but accurate), or by an extension of the Jinc function method (fast but possible inaccurate).

Further to this, being able to fully auralise the radiated signal would allow us to 'listen' to the response of a particular DML design, at some point in space. To listen to the radiated sound we need both phase and magnitude information, though the model gives only magnitude. If a minimum phase assumption is applied, we can regain the phase information by using the Hilbert transform.

5.3 Alternate Model

The response of DMLs has been found to be very smooth due to a high modal density, and so using the fast method of computing radiated power (by addition of driving point and reverberant field radiation) is a valid approximation. Currently this takes in the region of 15minutes to compute, due to using the (already fast) Jinc function method to calculate the radiation efficiency. If the direct method [Leppington et al, 1982] is used a tool which give the power spectrum in less than a second will be possible.

5.4 Panel Optimisation

One outcome of this project is a very fast method for computing the power spectrum of such a DML. With such a fast tool it is now possible to use optimisation in the design of DMLs. Possible criteria for optimisation include – total power output, critical frequency, modal density, and bandwidth of low frequency modal region. The latter of these criteria will need to use the full Jinc function based model, for the other three the fast SEA model will suffice. Parameters that can be included in optimisation procedures include damping, stiffness, panel dimensions, and boundary conditions. The possibility of using non-uniform plates and varying the drive point position is another area of investigation.

Section 6: Acknowledgements

Prof Robin Langley – for steering me in the right direction throughout the project

Tim Hughes – who saved me a great deal of time when using the laser vibrometer

Prof Jim Woodhouse – for use of his data logging and modal analysis MatLab program

Prof Malcolm Atkinson – for help conquering the subtleties of Word

Prof Frank Fahy – for a chance conversation that resulted in interesting analysis results

Marcel Leutenaggar – for an optimised sine function that speeded up MatLab by 2x

Gail and Mum – who harass me when I slip into procrastination mode

The Flat – for organised fun

Section 7: References

1. Azima, H (1998): '*NXT Technology – when a little chaos is good for you'*, originally published in Audio Magazine.
   Available at: http://www.emgeton.com/manual_speakers/NXT%20Technology.pdf
   [cited 16th May 2007].
2. Cremer L, Heckl M & Petersson B.A.T (2005): *'Structure Borne Sound'*, 3rd Edition, Springer-Verlag Berlin Heidelberg, Chapter 7 p. 454
3. Crighton D.G, Dowling A.P, Ffowcs-Williams J.E, Heckl M & Leppington F.G, (1992): '*Modern Methods in Analytical Acoustics – Lecture Notes'*, Springer-Verlag London Ltd, Chapter 20 p. 589
4. Elac Electroacoustics (n.d.): *'DML – Distributed Mode LoudSpeaker'*
   Available at: http://www.elac.com/en/products/imago/dml.html
   [cited 22nd May 2007]
5. Fahy F (1987), *'Sound and Structural Vibration'*, Academic Press London, pages 94 & 237
6. Hill N & Mapp P (2003): '*An overview of suitable measurement and assessment techniques for distributed mode loudspeakers',* The Journal of the Acoustical Society of America, Vol. 114, Issue 4, p. 2410
7. Langley, R (2007): *'Numerical evaluation of the acoustic radiation from planar structures with general baffle conditions using wavelets'*, The Journal of the Acoustical Society of America - Vol 121, Issue 2, p. 766-777
8. Leppington F.G, Broadbent E.G & Heron K.H. (1982): *'The Acoustic Radiation Efficiency of Rectangular Panel'*, Proceedings of the Royal Society of London. Series A, Mathematical and Physical Sciences, Vol. 382, No. 1783, p. 245-271.
9. Lyon, R (1975): *'Statistical Energy Analysis of Dynamical Systems'*, MIT Press, pages 49 & 234
10. Norton M & Karczub D (2003), *'Fundamentals of Noise and Vibration Analysis for Engineers'*, 2nd Edition, Cambridge University Press, Chapter 3 p. 210
11. Wharfedale n.d.: *'PPS1 DML product specification'*
    Available at: http://www.wharfedale.co.uk/model.php?model_id=55#
    [cited 25th May 2007]
12. Williams & Maynard (1982): *'Numerical evaluation of the Rayleigh integral for planar radiators using the FFT'*, The Journal of the Acoustical Society of America –Volume 72, p. 2020-2030

Section 8: Appendices

Appendix 1 *Description of Jinc Function*

The Jinc function is defined as:

$$jinc(x) = \frac{J_1(x)}{x},$$

where $J_1(x)$ is a Bessel function of the 1st kind and satisfies $\lim_{x\to 0} jinc(x) = \frac{1}{2}$.

The graph below displays a 1D jinc function for values of x from -15 to 15.

Figure A1 – 1D Jinc Function

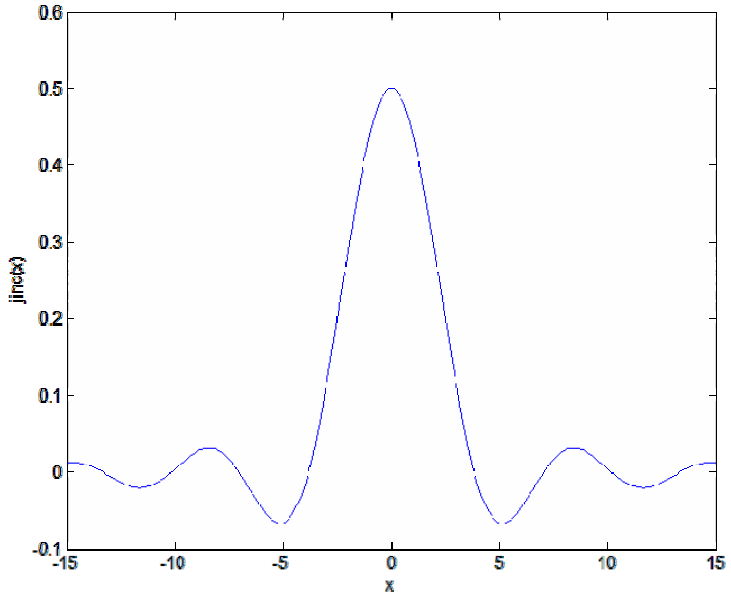

Appendix 2 Equations Used to Calculate Modal Parameters

Modal Density: $$n_d = \frac{L_x L_y}{4\pi}\sqrt{\frac{\rho h}{D}}$$

Critical Fequency: $$\omega_c = c_a^2\sqrt{\frac{\rho h}{D}}$$

Modal Overlap Factor: $$m_d = \omega\eta n_d$$

[Cremer & Heckl, 2005, p302 & 496]

Appendix 3 Mobility Transfer Function SEA Verification

Figure A2 – Mobility Transfer Function, Model predicted and SEA Approximation

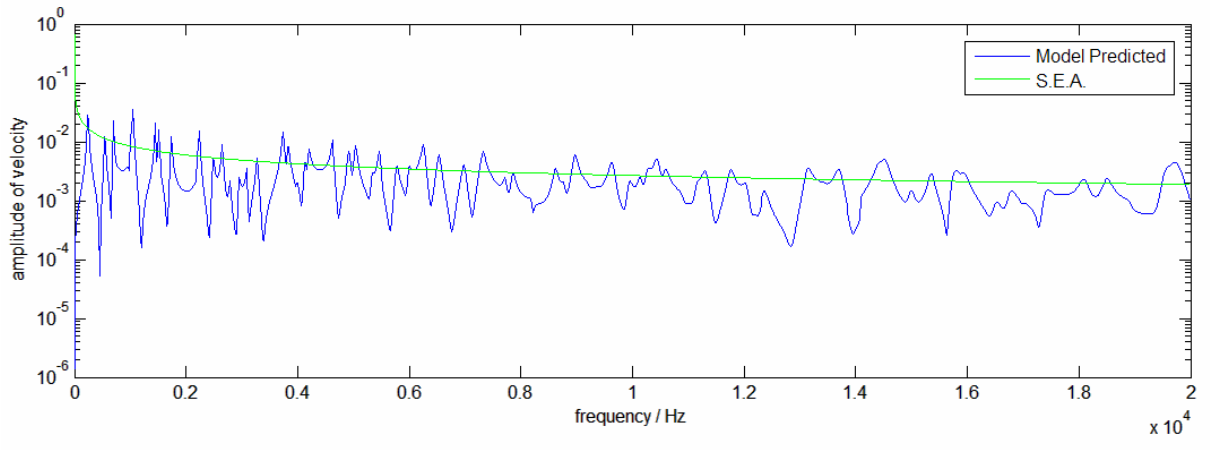

The SEA approximation for velocity is found using the following equation:

$$v_{SEA}(\omega) = \sqrt{\frac{\pi n_d}{2(\rho h L_x L_y)^2 \omega \eta}}$$

where n_d defines the modal density of the plate.

Appendix 4 make_R code printout

```
function R = make_R(Lx, Ly, c)

%makes an array R, which contains the distance between the i'th and j'th
%points in the vectorised form of the plate position.
%Lx, Ly, and c are used to define the grid, before vectorising.


[B,A] = meshgrid((0:c:Ly),(0:c:Lx)); %make meshes of x and y position

AB = A + B*i; %combine x and y position into singlematrix, defining the x
               and y coordinates of every mesh point as x + iy

AB = AB(:); %vectorise matrix into single row vector

ABmat = repmat(AB,1,size(AB)); %make vertical mesh of x and y positions

R = abs(ABmat - ABmat.'); %find distance between points


return
```

Appendix 5 Power Validation using Non-dimensional Radiation Efficiency

Figure A3 – Radiation Efficiency vs Non-dimensional Frequency

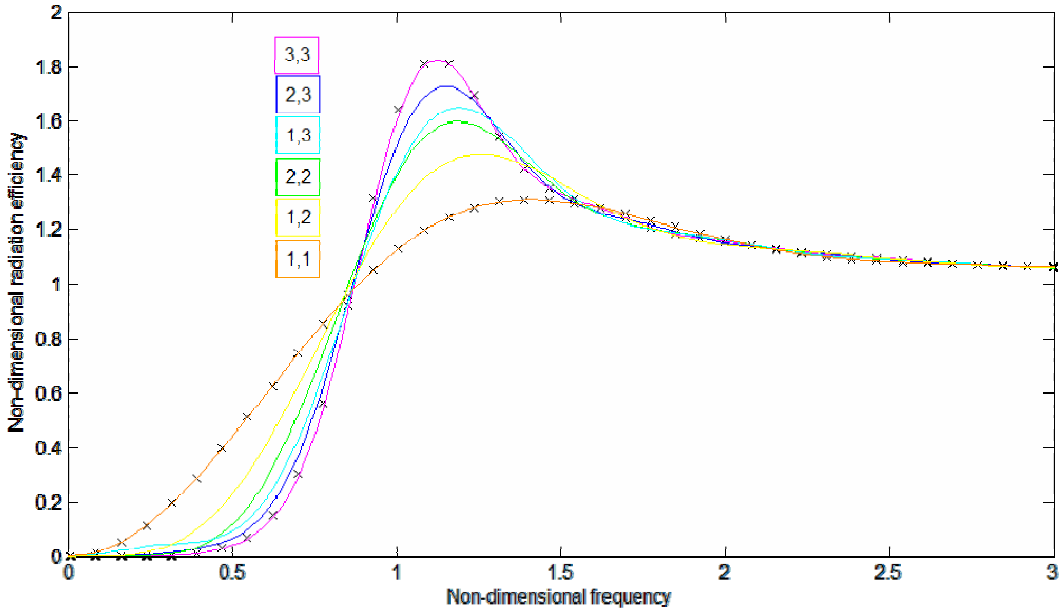

The above results are found using the Jinc function model, and are plotted atop benchmark results found using the FFT method of Maynard and Williams (marked with 'x'). FFT results kindly supplied by Prof. Langley. Excellent agreement is seen, validating the accuracy of the model.

Appendix 6 Experimental vs Predicted Transfer Function

Figure A4 – Mobility Transfer Function found using Model and Laser Vibrometer

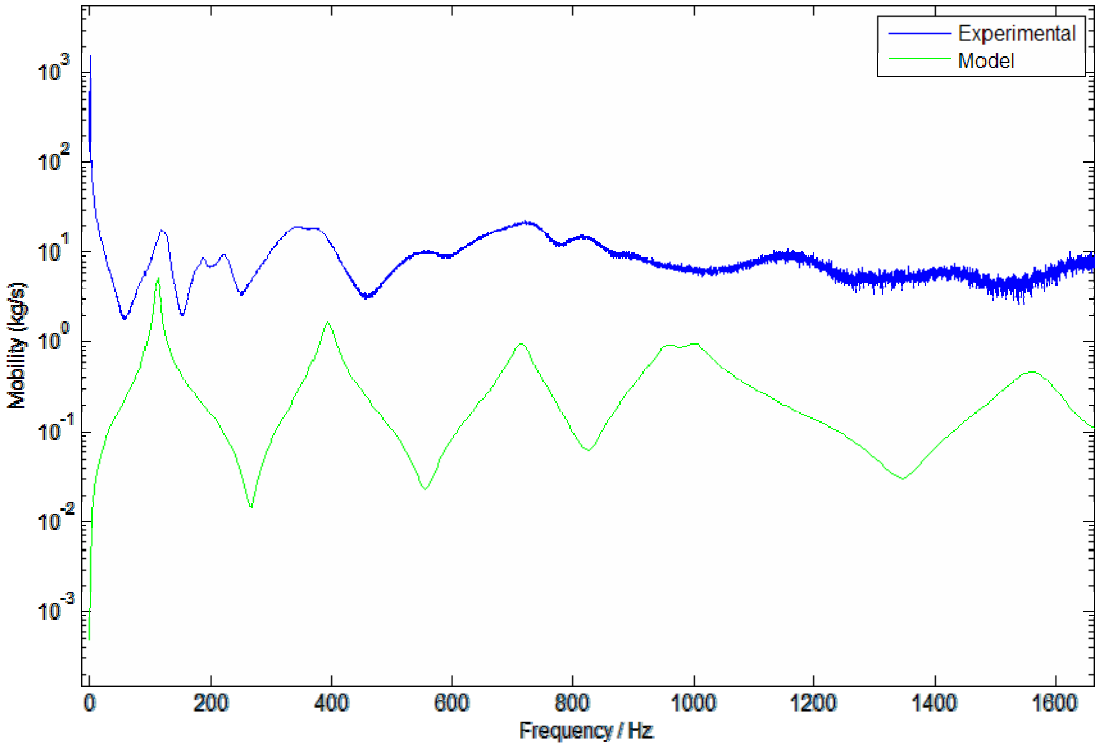

The first three model modes are predicted at frequencies coinciding with modes found experimentally. The model panel is excited exactly in its centre, but the experimental panel shows small resonances of anti-symmetric modes due to not being excited *exactly* in its centre. The experimental result comes from a laser vibrometer that was un-calibrated, hence we see an offset between the two spectra.

Appendix 7 Damping with frequency

Figure A5 – Fitting Curve to Experimental Damping Data

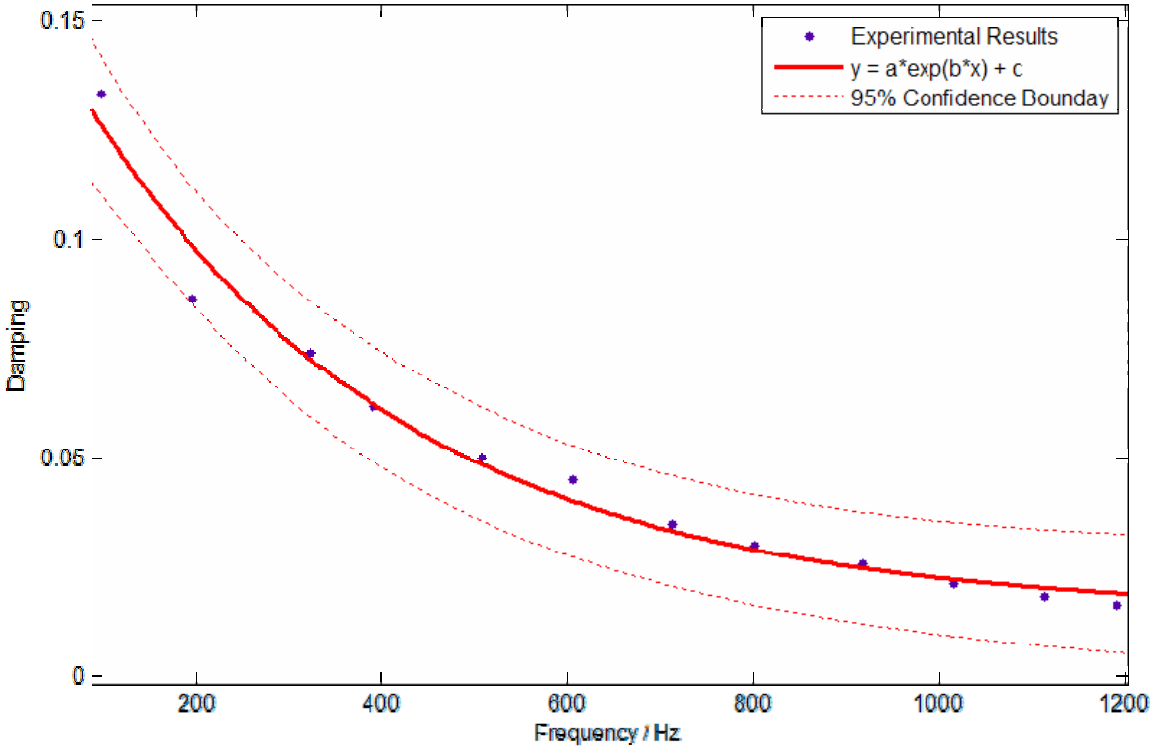

MatLab Curve Fitting Tool Output:

```
General model:
       f(x) = a*exp(b*x)+c
Coefficients (with 95% confidence bounds):
       a =      0.1487  (0.131, 0.1664)
       b =   -0.002897  (-0.003768, -0.002027)
       c =     0.01422  (0.003852, 0.02459)
Goodness of fit:
  SSE: 0.0002492
  R-square: 0.9811
  Adjusted R-square: 0.977
  RMSE: 0.005262
```

For a line of best fit that gives a high R^2 value we find that the asymptote, c, is at c = 0.014. This is an estimate for the internal damping of the panel.

Appendix 8 Theoretical Power Plots

Figure A6 – Power Spectrum for 95x65mm² Panel

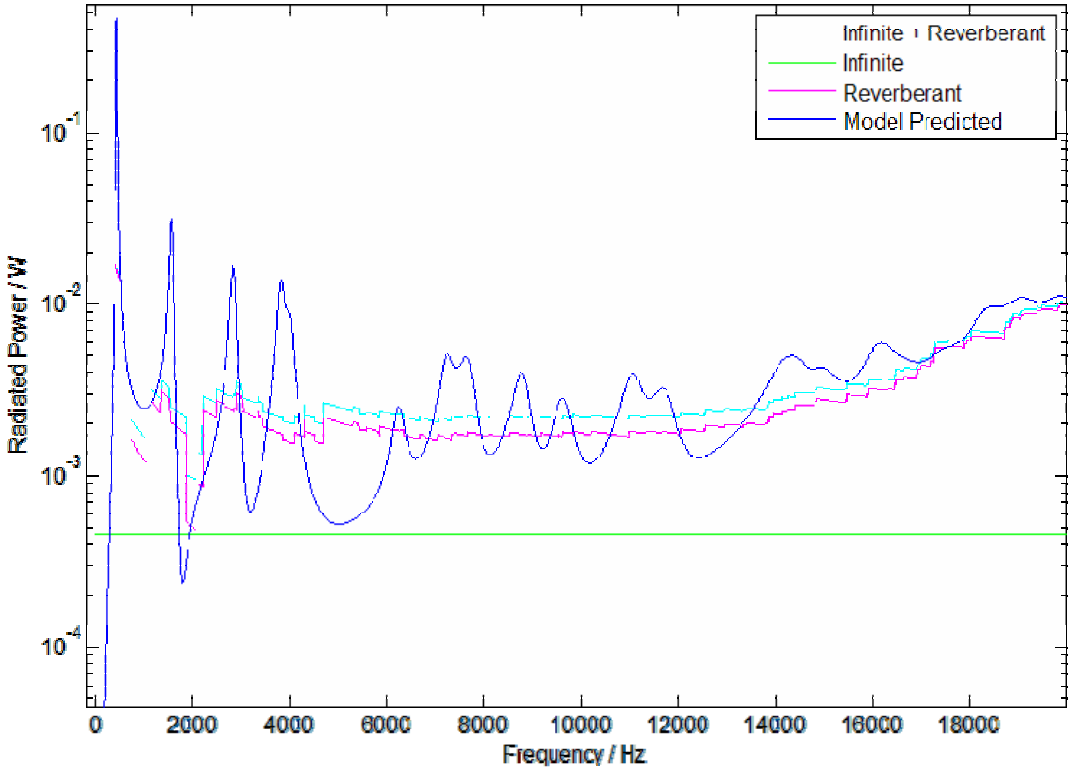

Figure A7 – Power Spectrum for Pane with 0.1x Stiffness